



High-Efficiency Dye-Sensitized Solar Cells: A Comprehensive Review

Ankit Stephen Thomas

Department of Chemical Engineering, National Institute of Technology Karnataka, Surathkal,
India

ankitstthomas@gmail.com

Abstract. Keeping in mind our community's dependency on non-renewable sources of energy, it is a gravitating issue that seeks our attention and requires us to switch to renewable sources of energy at the earliest. A Dye-Sensitized Solar Cell (DSSC) is a third-generation photovoltaic technology that has immense capability to become highly commercial in a few years. Along the same lines, it is necessary to highlight that current DSSCs have shallow lifetime values, stability and performance. The efficiency of current DSSCs and the need to tackle their choice of materials and long-term stability is a concern. Some of the highest recorded efficiency values are around 12%, and this calls for severe replacement of conventional DSSC materials, modifications in the device structure and molecules, and improvement in testing and scaling-up measures. This review article underlines an introduction to DSSCs, working principle, components, high-efficiency DSSCs, strategies to improve device performance, DSSCs research in India, the advantages and disadvantages of the device, and recent research on fruit and flower-based DSSCs.

Keywords: Dye-Sensitized Solar Cells, Solar Cell Materials, Third Generation Photovoltaics, High-Efficiency Dye-Sensitized Solar Cells, Solar Cells.

Introduction

The commercial photovoltaic technologies present in today's market are fabricated using inorganic materials that are energy and cost-intensive. Moreover, these are manufactured from materials such as CdTe, which are not that abundant in nature. Organic photovoltaics do not possess such an issue, but their low efficiencies are still a concern. Organic photovoltaics use a donor-acceptor system which is responsible for exciton generation. A Dye-Sensitized Solar Cell (DSSC) requires a dye/photoanode interface responsible for charge generation and an electrolyte responsible for dye regeneration. The spectral absorption properties of the dye can be modified by altering the dye properties.

In contrast, the charge transport and dynamics can be optimized by modulating the electrolyte and photoanode. DSSC is an economic and a soon-to-be commercial device with a promising future ahead. This comprehensive review article highlights the various high-efficiency dye-sensitized solar cells that have been fabricated. It also discusses the simple concepts of a DSSC, its working principle, the pros and cons of this remarkable device, and strategies to improve its performance. Moreover, since this topic is of budding interest, especially in India, the review throws light on the ongoing research about each component of a DSSC and specific important examples of fruit and flower-based dyes as a photosensitizer.

A DSSC is a low-cost solar technology belonging to the group of third-generation photovoltaics. It consists of a photosensitizer sandwiched between a redox electrolyte and a photoanode and the respective electrodes. The current version available of DSSCs is also known as a Grätzel cell. Along with being low-cost, the device can also be fabricated on flexible substrates and non-glass-

based systems. Unlike other photovoltaic technologies, the usage of expensive materials like Pt, Ag and Au has been removed with the introduction of DSSCs. Although this invention results in poor stability and performance compared to other energy sources, the price to performance ratio is theoretically comparable, if not better, than other sources.

The DSSC, when compared to Si-solar cell, is different in two unique ways. Firstly, in a Si-solar cell, the silicon solar cell behaves as an electron-hole pair generator and the charge separator using the built-in electric field. However, in a DSSC, only the photosensitizer behaves as the electron-hole source generator, whereas the photoanode and redox electrolyte behave as the charge separators. In a DSSC, since the dye molecules are tiny, we need to increase 'dye loading' or increase the thickness of the dye layer to increase light-harvesting efficiency. DSSCs are currently being heavily investigated, and studies on getting them to become more widespread have already been initiated [1]. The usage of quantum dots, solid-state electrolytes and modified electrodes are being considered, along with tandem devices to obtain higher photovoltaic outputs.

Working Principle of a DSSC

A few essential components of a DSSC are mechanical support coated with a conductive material, semiconductor photoanode, photosensitizer, redox electrolyte and counter electrode. TiO_2 is the commonly used photoanode because of its low cost, wide availability and little to no toxicity. Ru-based dyes are the common photosensitizers used, and triiodide/iodide is the used redox electrolyte.

The working principle is as follows where [2]:

- The absorption photon occurs at the sensitizer/photoanode interface.
- The electron generated is then injected into the conduction band of TiO_2 .
- The injected electron travels through the semiconductor network to reach the back contact, travelling through the external load.
- The redox mediator's role is to regenerate the excited sensitizer, which completes the circuit entirely.

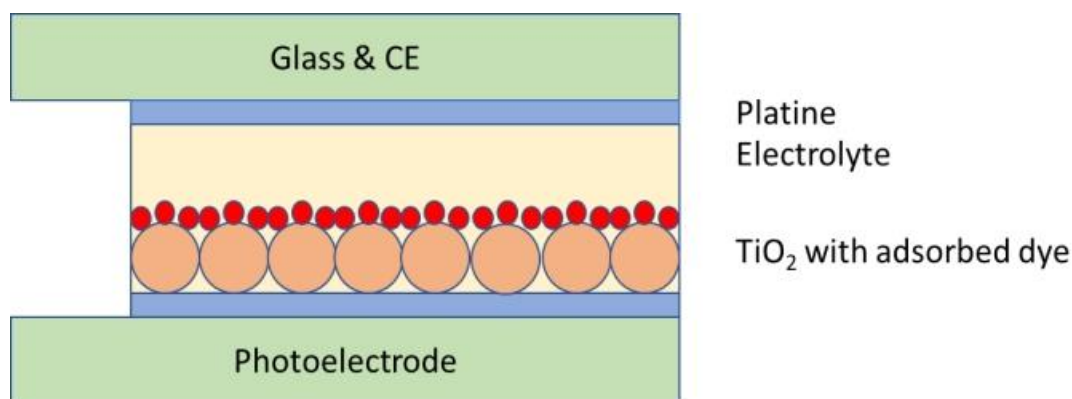


Figure 1. Schematic representation of a DSSC

However, this is only the working procedure for an ideal DSSC. There are some retarding reactions that occur that impact the DSSC negatively. Recombination effects are one such example. The efficiency of a DSSC is dependent on material/layer compatibility and the dye spectral ranges. The surface area and thickness of the semiconductor photoanode can be



increased to improve dye loading and light-harvesting efficiency. The monochromatic incident photon to current conversion efficiency (IPCE) is a property that defines the device's performance. It is defined as the ratio of the number of electrons generated by light in the external circuit and the number of excited photons (function of wavelength). The device's overall efficiency is defined as the ratio of the product of J_{sc} , V_{oc} and the fill factor to the intensity of intensity radiation. Fill factor (FF) is a value between 0 to 1 that throws light on the losses occurring in the device. The sensitizer and the device's photophysical and electrochemical properties dictate the device's performance. The oxidation potential is what sets the V_{oc} value. The electron transfer dynamics set the losses taking place in the cell.

The N3 and N719 dyes are the ones that are often used. The carboxylate group is the commonly used anchoring group. It coordinates the dye on the semiconductor surface to immobilize it. Since the anchoring group is bonded through a chemical procedure, it is bound to induce water into the device. This, in turn, impacts the long-term stability of the device. Hence, to eliminate this problem, it is crucial to have specific hydrophobic units or additives that can resolve this issue. Usually, alkyl chains are appended to the bipyridine chain with excellent hydrophobic properties. Moreover, these units show a maximum absorption at around 530 nm and display superior stability properties. It is important to note that the recombination effect should be suppressed as much as possible to attain maximum efficiency. The rate of electron transport and the injection process is of utmost importance to the overall efficiency. The excited electrons in the TiO_2 conduction band have a chance to recombine with the holes in the redox electrolyte to produce dark currents, which can impact the charge collection efficiency.

Techniques like surface passivation, insulating polymers, adding long aliphatic chains in the TiO_2 films, and spacer units between the TiO_2 and dye interface have reduced recombination. This can be because the aliphatic chains join laterally to form a network with the sensitizer, which makes it hard for the triiodide to reach the TiO_2 surface.

Recently, supersensitizers have been developed with a photosensitizer with high molar extinction coefficients and hydrophobic properties [2]. Examples such as adding thiophene units have excellent spectral absorption properties and shielding of redox electrolytes. As the extinction coefficients of the dye increase, the thickness of the photoanode can decrease. This further increases the V_{oc} value, improving performance and thus higher efficiency values.

Thiocyanate ligands are considered the delicate part of the device because of being a monodentate and ambidentate ligands. There have been studies to replace these ligands but unsuccessful because of shallow PCE values. YE05 is a dye developed by researchers with a high spectral response. Moreover, the IPCE values reach nearly 80% at 600 to 800 nm with high molar extinction coefficients. The presence of the fluorine atoms in the sensitizer modifies the redox potential to yield a $J_{sc} = 17 \text{ mA/cm}^2$, $V_{oc} = 800 \text{ mV}$, $FF = 0.74$ and $PCE = 10.1\%$. The YE05-based device also shows remarkable stability properties.

DSSCs are an invention closely related to the natural photosynthesis process. Efficiencies between 10 to 15% are easily attainable on a laboratory scale. However, further focus needs to be given to improving the J_{sc} , V_{oc} , stability and absorption values which can be improved by studying interfacial dynamics extensively.

Advantages and disadvantages of DSSCs



DSSCs are a third-generation of photovoltaics that have significant advantages compared to the conventional sources of solar cells. However, these devices come with their fair share of challenges which calls for more studies and research [1].

DSSCs can work under artificial or low-intensity light sources and effectively under cloudy or shaded conditions. Moreover, they can work from unorthodox angles, making them suitable for indoor applications as small-scale devices. The organic and inorganic materials used to fabricate a DSSC are very cheap. These further reduce the manufacturing costs compared to other solar cell technologies. The chemicals used in DSSCs are highly resistant. They possess mechanical and thermal stability, allowing these devices not rapidly to degrade under full illumination. In some cases, DSSCs can even work effectively up to 149 °F with negligible efficiency losses. It can be related to DSSC's use of a plastic substrate, allowing heat to radiate away quickly.

DSSCs have a low price to performance ratio, which does not make them suitable for commercialization at this stage. Compared to Si-based solar technologies, the efficiency is much lower as it mimics the natural photosynthesis process. The recombination effect is very prominent in a DSSC device, limiting its maximum performance. Lastly, liquid or other common electrolytes can lead to volatilization or leakage, leading to a safety issue. The sensitizer can also be mobilized on the photoanode surface due to poor contact in certain conditions, which further restricts the usage of DSSCs.

Examples of high-efficiency DSSCs

Benzothiadiazole dye for high-efficiency DSSCs

The best Dye-Sensitized Solar Cells (DSSCs) are considered highly efficient if they have an average Power Conversion Efficiency (PCE) between 10 to 14.2%. DSSCs have been comparatively poorly performing compared to photovoltaic technologies like PSCs or BHJSCs. The stability shown by this particular technology is relatively superior. These stability characteristics can be even subject to variation when non-volatile electrolytes are used. The stability under harsh conditions is improved up to 10 years of long-term performance.

Moreover, DSSCs provide consumers with an aesthetic appeal and lower toxicity. Currently, the conventionally used dyes are Ru-based dyes. These photosensitizers' expensive and toxic nature calls for alternative and efficient materials. Strategies like donor-(π -spacer)-acceptor, organic, electron-withdrawing and chromophores have been used for their unique optoelectronic properties. A previously reported dye using a benzothiadiazole unit (RK1) showed superior stability with a champion PCE of 10.12%. In this work, Godfroy and coworkers fabricated a dye based on a similar concept to generate a benzothiadiazole-based dye called YKP-88, where the TPA unit and thiophene ring are bridged [3,4].

The ultimate goal of fabricating photosensitizers is to shift the absorption range of the materials towards the visible range. The possible strategy could be to play on the pull-push effect by varying the electron-donating groups, the planarity of the molecules or π -conjugation systems. Thus, 4 dyes were produced, namely, YKP-137, MG-207, DJ-214 and MG-214. The former 2 dyes were produced by varying the TPA unit with alkoxy groups, and the latter 2 dyes were produced by swapping the benzene spacer with a furan unit. The optical properties of all the dyes are estimated using a dilute solution of dichloromethane. All the dyes show notable absorption in the visible



range, with molar extinction coefficients varying from 2.7 to 4.33×10^{-4} L/mol cm. The lower energy band is due to Internal Charge Transfer (ICT), and the other bands are due to π - π^* transition.

YKP-137 has a red shift of 28 nm compared to YKP-88. MG-207 has a shift of 3 nm, with the previous molecular changes having no impact on the absorption. However, the shift was more pronounced for the DJ-214 and MG-214 dyes due to the furan unit. In this case, using a furan unit improved the planarity of the molecule with nearly 0° in dihedral angle and improved anchoring ability. The furan unit produced an absorption shoulder between 400-450 nm. The dyes showed colors ranging from violet to blue in solution. The absorption spectra were further analyzed by anchoring these dyes on a TiO_2 layer (2 μm). The absorption spectra widened with a notable blue shift when all the dyes were anchored on the TiO_2 surface. This is due to the sudden carboxylic acid deprotonation function and the aggregate formation due to a furan unit.

The optoelectronic properties of the materials were studied through cyclic voltammetry (CV) measurements. The reversible oxidation potentials for MG-207 and MG-214 are around 0.45 and 0.95 V. YKP-137 is a much easier material to oxidize due to the alkoxy units showing oxidation potentials at 0.28 0.86 V. The HOMO levels for all the materials were nearly around -5.25 eV except for YKP-137 which was around -5.08 eV. The reduction potential for the YKP-88 and YKP-137 dyes are found to be similar, around -1.55 V. These potentials change on varying the π -conjugation units. The reduction potentials for MG-207, DJ-214 and MG-214 were -1.50, -1.45 and -1.40 V, respectively. The LUMO levels for 3 dyes lie in the range of -3.26 to -3.30 eV, and the dye with a benzene spacer has a more negative value. The practical analysis of the energy bands shows that the bands lie for adequate charge transportation between the TiO_2 and iodine/iodide electrolyte.

The DSSCs were manufactured and tested using a solar simulator under AM 1.5G and 1000 W/m^2 irradiation. The devices were manufactured using a liquid electrolyte and an ionic-based electrolyte. Thick electrodes are used of approximately 10-14 μm -thick along with 3-4 μm -thick reflecting layers. A thin mesoporous layer of TiO_2 is used to behave as an anchoring layer, ETM and passivating effect. The photovoltaic performances obtained from all the devices were made to be compared with RK-1 as a reference dye. The PCE values ranged from 7.01 to 9.78% with liquid electrolytes of low viscosity, with J_{sc} values more significant than $14.05 \text{ mA}/\text{cm}^2$. The dyes having a phenyl spacer exhibited better performance than furan spacers. However, the V_{oc} values of these dyes were comparatively lower. YKP-88, YK-137 and MG-207 showed V_{oc} values equal to 708, 726 and 704 mV, respectively. Whereas for DJ-214 and MG-214, the dyes were lowered by around 40-60 mV. The highest V_{oc} , as expected, was by YKP-137 due to its reduced recombination rate because of the alkoxy chains.

The lower V_{oc} values can be attributed to the higher recombination rates and the misalignment in the conduction band (lower). As per reports, substituting phenyl-hexyl groups of spiro carbon of the indene unit reduces the dye aggregation. To validate this particular finding, DSSCs were fabricated with and without CDCA. CDCA is an additive/adsorbent that removes the dye aggregates on the TiO_2 surface. The External Quantum Efficiencies (EQE) measurements were taken. The derived dyes exhibited a more excellent absorption response at longer wavelengths when compared to YKP-88. Moreover, the furan spacer dyes are less efficient in converting photons to electrons, and MG-207 showed the best performance under this criterion.



The performance of all the DSSCs can be reported as follows, the YKP-137 and MG-207 devices with iodine-liquid electrolytes had comparable PCEs to YKP-88. However, the usage of dyes like DJ-214 and MG-214 showed a detrimental impact on the performance of DSSC. When the liquid electrolyte was replaced with an ionic-based electrolyte, the J_{sc} values of all the dyes were above 15.4 mA/cm^2 , with DJ-214 and MG-214 dyes having 7.3% efficiency. The furan spacer's device possessed a PCE between 6.52 and 7.52% with varying electrolytes. The stability of all the devices was studied when they were exposed to 1000 W/m^2 at $65 \text{ }^\circ\text{C}$ under ambient conditions. The DSSCs were encapsulated using epoxy and a UV-absorbing polymer. After 1000 hours, the devices retained nearly 85% of their initial PCE. The YKP-88 device retained nearly 80% of its PCE after 291 days with a T_{80} value of nearly 7 years.

Co-sensitization of dyes is an innovative strategy to improve this photovoltaic technology's PCE levels and reliability. The mesoporous TiO_2 layer was used as an anchor to embed the dyes on its surface to design a co-sensitized device. This strategy can improve V_{oc} levels and reduce charge recombination to improve photovoltaic performance further. The dyes used in this case are YKP-88 and YKP-137, which are essentially the same structure but with variations in the alkoxy units. The bulky groups of TPA protect the TiO_2 surface and further reduces charge recombination of the redox electrolyte. YKP-88/YKP-137 dyes were made to vary in the ratio of 8/2 and 2/8 along with a 5 mM of CDCA. The photovoltaic performance of the device is recorded to be J_{sc} of 20.66 mA/cm^2 , V_{oc} of 745 mV, FF of 71% and PCE of 10.9%. It is important to note that the performance obtained from the co-sensitized device was much improved relative to the single dye devices.

Along with an improvement in J_{sc} , there was a significant improvement in V_{oc} , which improved the device's performance. The Transient Photovoltage (TPV) measurements show that the co-sensitized device has a higher charge density when compared to its single-dye counterparts. Moreover, the electron lifetimes measured in the co-sensitized device were higher than in the single dye device. The IPCE measurements show a correspondingly higher photon-to-electron conversion efficiency and response to the NIR region for the co-sensitized device.

The devices with 4 different dyes showed reasonable PCE between 6.52 to 7.52%, with excellent stability characteristics of nearly 85% retention after 1000 hours. Even fabricating a co-sensitized device proves to be an effective tool for developing commercial DSSCs. These dyes can be implemented for large-area devices (14 cm^2 active area), thus, showing the future of organic dyes in emerging photovoltaic technologies.

Indoline metal-free dyes for DSSCs

The conventionally used dyes for DSSCs are Ru-based dyes, typically reported as N719. There is a pressing need to transition to metal-free-based dyes that are eco-friendly, readily producible, and have suitable photovoltaic properties. The previously reported Indoline-based dyes produced specific photovoltaic results. However, the low bandgap and variation in HOMO, and LUMO levels with an increase in methine chain length, produced a redshift in the absorption spectra. In this section, Horiuchi and coworkers fabricated 4 dyes with nearly similar molecular backbones under identical conditions [5].

The essential molecular backbone is similar. Only a variation in R_1 , R_2 and R_3 molecules produced the 4 different dyes, as shown in Table 1.

Table 1. Molecular structures of Indoline 1-4 dyes [5]

| Dyes | R ₁ | R ₂ | R ₃ |
|------|---------------------------------------|----------------------------------|---|
| 1 | -CH ₂ COOH | -CH ₂ CH ₃ | =S |
| 2 | -CH ₂ COOH | -CH ₂ COOH | =S |
| 3 | -CH ₂ CH ₂ COOH | -CH ₂ CH ₃ | =S |
| 4 | -CH ₂ COOH | -CH ₂ CH ₃ | =C ₃ S ₂ ON-CH ₂ CH ₃ |

The absorption spectra of the Indoline 1 dye were recorded on a TiO₂ electrode. The results showed 2 revealing peaks at 526 and 541 nm, respectively. The molecular coefficient for the Indoline 1 dye was found to be 68700 M⁻¹cm⁻¹ at 526 nm. These obtained values were much higher when compared to the molecular coefficient of 13900 M⁻¹ cm⁻¹ at 541 nm for N3 dye. In this section, each dye is represented along with the letter 'N'. The N2 and N3 dyes show similar absorption characteristics to N1, with an absorption peak at 532 and 531 nm, respectively. The more significant number of rhodanine rings on N4 depicted a redshift in its absorption. The colours of the dye also vary from blue to purple to black for the 4 dyes on the TiO₂ electrode. There was a slight change in absorption range whenever the dye was anchored on the TiO₂ electrode, indicating some chemical/physical reaction occurring between the dyes and TiO₂.

The DSSC device was fabricated using 2 kinds of electrolytes, following the architecture: Pt/TiO₂/Dye/electrolyte/FTO. Here the electrolytes used are Lil and 4-tert-butyl pyridine (TBP). A solar simulator recorded the photovoltaic performance at AM 1.5 G and 100 mW/m². The solar-to-electric conversion efficiency of all 4 dyes was much higher than other metal-free organic dyes that have been used previously. The IPCE measurements showed 85% from 445 to 600 nm for the N1 dye. Similarly, N4 dye showed an efficiency greater than 60% in the range from 415 to 510 nm. Moreover, these dyes display large photocurrent values with large IPCE values. The obtained photovoltaic output parameters are summarized in Table 2.

Table 2. Photovoltaic Performance of Indoline dyes compared to N719 reference dye [5]

| Dye | V _{oc} (mV) | J _{sc} (mA/cm ²) | PCE (%) | FF |
|------|----------------------|---------------------------------------|---------|------|
| N1 | 645 | 18.75 | 0.538 | 6.51 |
| N2 | 584 | 17.50 | 0.538 | 5.50 |
| N3 | 628 | 17.38 | 0.513 | 5.60 |
| N4 | 569 | 19.56 | 0.533 | 5.93 |
| N719 | 754 | 16.68 | 0.657 | 8.26 |

Additives like cholic acid derivatives such as chenodeoxycholic acid are used to improve N1-DSSC performance. It has been reported that cholic acid derivatives prevent the aggregation of dye molecules on the TiO₂ surface. It is shown that N1 dye with a cholic acid additive at an optimal concentration (20 mM) results in twice the better performance. To improve electrolyte composition, 0.05 M of TBP solution was ideal for N1 DSSC. Moreover, on varying the group iodides used as an electrolyte like Lil, NaI, KI, Cel and (n-butyl)₄NI, the Lil variant shows the most attractive photovoltaic performance. The optimal performance of the best DSSC can be summarized as follows using the following criterion a) N1 dye concentration = 5 x 10⁻⁴ M and Chenodeoxycholic Acid concentration = 1 x 10⁻³ M b) Electrolyte Iodide mixture = 0.1 M Lil and 0.05 M TBP. On conducting TG-DTA analysis, N1-based DSSC showed superior thermal stability till 300 °C. It is important to note that the photovoltaic performance obtained from this modification is the highest efficiency value for metal-free organic DSSCs without an anti-reflecting layer.



Isophorone dyes for high-efficiency DSSCs

The most efficient sensitizers are of the D- π -A form. D and A represent donor and acceptor molecules, respectively, and π represents the conjugation system. It is important to note that the D or donor molecules are of utmost importance because they dictate the energy band alignment of the absorber molecule. Thus, having a suitable donor molecule can directly impact photovoltaic performance, driving forces, absorption characteristics and spectral properties. The appropriate usage of π -systems can further cause a redshift in absorption. It is essential to highlight that extensive π conjugation can lead to dye stacking on the TiO₂ surface. The greater the π -stack, the electron injection capability reduces. Additives like deoxycholic acid (DCA) reduce dye aggregation on the TiO₂ surface. Previous reports have shown how para-bis-substituted aniline was used to modify NKX-based dyes on coumarin derivatives. Hara et al. showed how incorporating alkyl chains on oligothiophene units could reduce molecule aggregation and charge recombination probability [4].

Like this process, Bo Liu and coworkers used an isophorone unit for the π -cyclohexene bridge. Thus developing 3 dyes, D-3 and 2 reference dyes, D-1 and D-2, Here indoline, dimethylphenylamine and triphenylamine units are used as donor molecules, respectively.

D-1 and D-2 have decent absorption characteristics, but introducing the indoline unit shows a considerable red-shift with the absorption range broadening in the visible region and the λ_{\max} shifted to 497 nm. The molar extinction coefficient of D-3 at λ_{\max} is $3.76 \times 10^4 \text{ M}^{-1}\text{cm}^{-1}$ whereas for D-1 and D-2 dyes, the values are 3.27×10^4 and $2.69 \times 10^4 \text{ M}^{-1}\text{cm}^{-1}$, respectively. When these values are compared to N719 dye, the molar extinction coefficient is $1.47 \times 10^4 \text{ M}^{-1}\text{cm}^{-1}$ at 535 nm, which is comparatively inferior to D-3. On anchoring the dyes onto the surface of TiO₂, the λ_{\max} is slightly blue-shifted. The adsorption threshold is shifted by more than 50 nm from 650 nm to 700 nm. These can be attributed to the interaction of the carboxylate group with TiO₂. The LUMO levels of the dyes are calculated and found to be -0.71, -0.84 and -0.85 V for D-2, D-1 and D-3, respectively. These values are more negative than the CBM of TiO₂, which allows effective and suitable electron injection. The orbital energies were also calculated using a hybrid density functional theory where the LUMO energies were found to be -2.15, -1.98 and -2.16 V for D-1, D-2 and D-3 dyes, respectively. The best performing (D-3) device was fabricated with and without DCA to validate the phenomenon of dye aggregation. On adding 1.0 mM of DCA solution to an acetonitrile solution of D-3, the photocurrent decreased from 14.76 to 11.07 mA/cm². These values show that there was no significant π -aggregation for the D-3 dye. The reasons for this can be multiple such as the twisted isophorone unit, an indoline unit, non-planar ground state geometry, and the two methyl groups in the isophorone unit contribute to the steric hindrance of the molecule. From the above reasonings, the D-3 dye generally prevents close π - π aggregation. The performance of devices is analyzed with varying thickness of TiO₂ electrodes. The thickness used in this particular scenario is 2.2, 3.4, 3.8, 5.0 and 6.7 μm . Although the FF values remained constant in all cases, the J_{sc} values increased from 11.19 mA/cm² to 18.63 mA/cm². However, the V_{oc} values decreased with the increasing thickness of TiO₂. This can be attributed to the increase in the TiO₂ area, which provided a higher charge recombination probability. The usage of thick TiO₂ did not permit much light permeation into the device, which further prevented charge excitation and thus led to lower V_{oc} values. This counter-current effect generated a nearly constant value of PCE, with a maximum PCE of 7.41% at 5.0 μm . The IPCE spectra of the 3 dyes are analyzed concerning N719. The high absorption properties in the broad region produced a higher efficiency value for D-3 than D-1 and D-2, which exceeds 80% in the range of 430-630 nm. This value reached a maximum efficiency of 89% at 508 nm. The integrated short-circuit current



obtained is nearly 18.63 mA/cm². It is important to note that the conversion efficiency values obtained for the D-3 are much higher than in the case of N719.

The performance of the D-3 dye-based device can be summarized as follows: J_{sc} of 18.63 mA/cm², V_{oc} of 634 mV, FF of 0.63 and PCE of 7.41%. When comparing this performance for the N719-based device, the J_{sc} value was only 15.60 mA/cm² with a PCE of 7.03%.

Thus, we can firmly conclude that in a D- π -A system, the D atom plays a vital role in determining the photophysical, electrochemical and photovoltaic performance of the device and film produced. Moreover, the results that are produced through these molecular configurations are higher than conventionally used dyes, which provides researchers with a potential commercial candidate.

Porphyrin sensitizer for 14.2% DSSC

The molecular structure of the dye predominantly dictates the performance of a DSSC. Conventionally, Ru-based dyes have been used, but organic sensitizers and Zn-porphyrin complexes have DSSC implications with recent innovations. Yao et al. showed how a dithienopicenocarbazole organic dye (C281) could produce a PCE of 13% in the presence of Co(bpy)₃^{2+/3+} electrolyte. Similarly, Kakiage et al. produced a PCE of 14.34% using a co-sensitized device with ADEKA-1 and LEG-4 using co-adsorbents like Co(phen)₂^{2/3+} electrolyte. However, it is essential to note that PCE levels are just one aspect of commercial DSSCs. It is essential to understand that factors like long-term stability, cost efficiency, material availability, and novelty are essential too. The D- π -A has been the most widely regarded photosensitizer configuration due to its efficient intramolecular charge transfer (ICT). Increasing research has been going on that requires the discovery of novel and new D and A molecules along with π moieties. The dyes used in the works of Jung-Min Ji and coworkers highlight asymmetric thieno[3,2-b]benzothiophene moiety and 4-hexyl-4H-thieno[3,2-b]indole (HxTI) moiety into dye backbone as new π -bridges [6]. The dyes referred to in this particular case are SGT-130 and SGT-137. In addition to this, 4 different fluorene-based donors are studied, namely, FA, HFA, DFA and BBFA, to produce dyes referred to as SGT-146, SGT-147, SGT-148 and SGT-149.

The UV-Vis absorption measurements of the SGT sensitizers are analyzed in THF solutions. The dyes show two distinct absorption bands around 360-400 nm that account for the π - π^* transition of the D molecule, whereas the second band between 500-600 nm is due to the ICT between D and A. The maximum absorption wavelength (λ_{abs}^{max}) of nearly all the dyes is red-shifted with maximums at 343, 377, 380, 381 and 389 nm for SGT-137, SGT-146, SGT-148, SGT-147 and SGT-149 dyes respectively. By comparing the above values, we can clearly conclude that the fluorene donors show a significant red-shift in values, even reflected in the $\lambda_{max, abs}$ values. Thus, we can conclude that the usage of fluorene can improve the light absorption capacity at shorter wavelengths. The conjugation length in the D moiety also significantly impacts the molar extinction coefficient by giving a more extreme value. The fluorene unit has improved the intramolecular electron push-pull effect on the D- π -A unit. The CV results of the SGT dyes show a calculated value for the first oxidation potentials (E_{ox}) as follows, 0.86, 0.77, 0.77 and 0.84 V for SGT-146, SGT-147, SGT-148 and SGT-149 dyes respectively. The first quasi-reversible oxidation corresponds to the HOMO levels following the trend BBPA < FA < BBFA < HFA \approx DFA.

The SGT sensitizers have energy bands sufficiently higher than liquid electrolytes Co(bpy)₃^{2+/3+} and ionic electrolytes like I⁻/I₃⁻ which is thermodynamically favourable. Moreover, a similar alignment can be observed in the LUMO levels of the SGT dyes, which are placed above the TiO₂



conduction band, which ensures beneficial electron injection properties. On calculating the dihedral angle of the dyes, all the SGT dyes showed a similar value between the D and HxTI units. The value was found to be nearly equal to 42° . It is important to note that the BBFA has a rotatable dialkoxy phenyl unit with the dihedral between the fluorine and dialkoxy unit 42° . The HOMO level is delocalized among the HxTI π -bridge and the D unit. The HOMO-1 level extends to the BTD-phenyl unit, and finally, the LUMO level extends to the A unit. Some visible overlapping effects may be observed related to the ICT between D and A units to indicate effective charge transfer and separation. It is important to note that the theoretical values of HOMO/LUMO levels, absorption spectra and donor strength (BBPA < FA < BBFA < HFA \approx DFA) match very well with the experimental values. Replacing the BBPA unit with FA, BBFA, HFA, and DGA increases the HOMO-1 orbitals by 2 times, and the π -bridge contribution to the HOMO-1 orbital is decreased. On decreasing the planarity of the D unit, there is a significant red-shift observed. However, there is a consequent decrease in ICT intensity.

The photovoltaic output parameters were analyzed using 2 redox electrolytes under AM 1.5 G ($100\text{W}/\text{m}^2$) with a metal mask of 0.041 cm^2 . The volume ratio varies concerning solvents, coadsorbents, counter anions, and dye concentration. To determine the optimum performance of a DSSC device. On varying the unit from biphenyl to fluorenyl, the solubility levels changed, which further impacted the volume ratio of the dipping solvents. These produced lower PCE levels for SGT-137. The PCE levels of the SGT device with CDCA is 9.5%, 3.6%, 8.0%, 7.9% and 11.2% for the SGT-137, SGT-146, SGT-147, SGT-148 and SGT-149 dyes respectively. On changing the coadsorbent from CDCA to HC-A1, the PCEs of the dyes further changed to 10.0%, 9.3%, 9.6%, 10.0% and 10.3%, respectively. Analyzing the SGT-146 dye individually, we can see a dramatic increase in PCE when the coadsorbent is changed to HC-A1 because of the alkyl chain absence in its donor unit. The counter anion was also changed from $(\text{B}(\text{CN})_4)$ to TFSI, where all the SGT-dyes showed an increase in PCE values ($> 10\%$). The best PCEs were obtained from devices using HC-A1 coadsorbent, $\text{Co}(\text{bpy})^{2/3+}$ redox electrolyte and EtOH/THF dipping solvents. For the $\text{Co}(\text{bpy})^{2/3+}$ electrolyte, the PCE's are as follows: 10.5%, 10.2%, 10.5%, 10.6% and 11.4% for SGT-137, SGT-146, SGT-147, SGT-148 and SGT-149 dyes respectively. The best performance was obtained from the SGT-149-based DSSC. This had a BBFA donor with a $V_{oc} = 0.909\text{ V}$, $J_{sc} = 17.6\text{ mA}/\text{cm}^2$ and $\text{FF} = 73.2\%$ with an HC-A1 as a coadsorbent. The excellent performance of this dye can be attributed to the bulky nature of BBFA, high molar absorptivity and dye absorption amount. Thus, it is reasonable to conclude that as the nature of the bulky substituent decreases, the V_{oc} decreases. The J_{sc} values increase in a trend, 16.39, 16.67, 17.15, 17.12 and 17.49 mA/cm^2 for SGT-137, SGT-146, SGT-147, SGT-148 and SGT-149 based dyes respectively. The IPCE spectra can also be correlated to the performance of the device. Similarly, devices with low J_{sc} values showed a low IPCE value, and the SGT-149 dye with the highest J_{sc} showed a high IPCE value. SGT-137, SGT-147 and SGT-148 have similar absorption ranges. On varying the electrolyte to I^-/I_3^- , the J_{sc} value for SGT-137, SGT-146, SGT-147 and SGT-148 was 18.4-18.7 mA/cm^2 . The highest J_{sc} (19.32 mA/cm^2) was for SGT-149 dye. On conducting a light-soaking test with devices containing both the electrolytes, most devices retained 84-88% of their initial PCE after 1000 hours of light soaking. The TRPL measurements were taken on TiO_2 and Al_2O_3 , where the decay lifetimes were 27.3, 27.5, and 22.7 ps for SGT-146, SGT-147, SGT-148, SGT-149 dyes, respectively, on TiO_2 . Similarly, on Al_2O_3 , it was found to be 429.5, 286.9, 335.9 and 327.2 ps. The electron injection efficiency η_{inj} values are 93.6, 90.3, 93.5 and 92.4%, respectively.

The EIS measurements are taken and the $\text{Co}(\text{bpy})_3^{2+/3+}$ based DSSCs had a R_{rec} values of 22.41, 29.03, 29.61, 34.07 and 72.59 Ω for SGT- 146, SGT-137, SGT-147, SGT-148 and SGT-149 dyes



respectively. These values correspond very well with the trend seen in V_{oc} values. Even the T_r and C_{μ} values followed the same trend as the R_{rec} values. The T_r values were 17.4, 17.9, 18.1, 18.9 and 22.7 ms, which is by the V_{oc} and R_{rec} values. The η_{col} values were found to be 78.6%, 75.8%, 78.7%, 78.8% and 83.7% for SGT-137, SGT-146, SGT-147, SGT-148 and SGT-149 dyes respectively. A similar T_r and R_{rec} values trend are seen for the I^-/I_3^- electrolyte-based DSSCs. The C_{μ} values were found to be in the order SGT-146 < SGT-147 \approx SGT-137 < SGT-148 < SGT-149. The η_{col} values from EIS were found to be 78.6%, 75.8%, 78.7%, 78.8% and 83.7% for SGT-137, SGT-146, SGT-147, SGT-148 and SGT-149 respectively. These results show that SGT-149 (BBFA) has the best characteristics for efficient DSSCs, which produce high V_{oc} because of the BBFA unit and a high J_{sc} unit because of the umbrella effect.

A strategy was then used to develop a co-sensitized device using a porphyrin-based dye (SGT-021) and SGT-149. The necessity for employing SGT-021 is to compensate for the weak absorption properties of SGT-149 in the range of 430-510 nm and 680-800 nm. Two devices were fabricated using $Co(bpy)_3^{2+/3+}$ and I^-/I_3^- electrolytes. Using the former electrolyte, the photovoltaic parameters obtained were, PCE = 14.2%, V_{oc} = 0.919 V, J_{sc} = 21.06 mA/cm² and FF = 73.4%. Using the latter electrolyte, the photovoltaic parameters obtained were, PCE = 11.6%, V_{oc} = 0.738 V, J_{sc} = 22.25 mA/cm² and FF = 70.9%. The I⁻ ratio for SGT-021 and SGT-149 is 1:3 and 1:3.5 for Cobalt and iodine-based electrolytes. On analyzing the IPCE spectra, the weak absorption properties of SGT-149 are compensated by SGT-021, which is reflected through the high J_{sc} values. The R_{rec} , T_r and η_{col} values for the Co electrolyte are 69.8 Ω , 29.23 ms and 98.5% and for the Iodine electrolyte are 22.98 Ω , 670.3 ms, 90.1%, respectively. The high V_{oc} values can be justified through the favourable R_{rec} and T_r values, whereas the high η_{col} justifies the high IPCE value. On analyzing the Co-based co-sensitized DSSC under AM 1.5 G at 50 °C, the device retained nearly 80-83% of its initial PCE after 1000 hours of light-soaking.

This particular study analysed how 4 new HxTI-organic dyes using the D- π -A configuration can help generate efficient DSSCs. Moreover, incorporating fluorene-based substituents further improved the stability of the DSSC under light-soaking tests. Lastly, the co-sensitization of suitable dyes (SGT-021 and SGT-149) led to a substantial increase in V_{oc} and J_{sc} to produce devices with more than 10% PCE levels which is a suitable candidate for commercial applications.

Robust organic dye for stable and efficient DSSCs

A suitable and appropriate dye is essential as that is the critical component that generates charge carriers and permits the suitable transportation and injection of electrons. It is also essential to regulate the TiO_2 /dye/electrolyte interface as a rough or incompatible interface can increase interfacial recombination. Thus, it is necessary to investigate suitable dyes on a laboratory scale and examine the possible mechanisms to scale such technologies. The conventional Ru-based sensitizers are not earth-abundant, raising the cost of the device. Moreover, some Ru-complexes with a broad absorption range often show modest molar extinction coefficients, limiting the device's performance. Looking into organic sensitizers is of great importance because of their lower costs, more accessible synthesis, larger extinction coefficient values and reasonable stability values. Metal porphyrins are a good option, but the complex synthesis procedure, low product yields, and difficulty anchoring require less complex approaches. In this section, Damien Joly and coworkers synthesized a dye known as RK1, which follows a simple 5-step synthesis process from low-cost precursor solutions [7]. The main aim was to use a dissymmetric π -conjugated bridge with alkyl chains, electron-deficient groups, and an electron-rich group.



The thiophene BTD phenyl chromophore implies the π -bridge corresponding to the D- π -A configuration. Taking the UV-Vis absorption measurements, the RK1 sensitizer shows two significant absorption bands. Firstly, the one located in the UV region can be attributed to the π - π^* transition corresponding to the aromatic rings. Secondly, the one located in the visible region can be attributed to the ICT transition between electron-donating and withdrawing groups of the entire sensitizer molecule. The measurements of these devices were done regarding N719-based conventional dye.

The molar extinction coefficient of RK1 is twice as high as N719 at 470 nm, which is also responsible for its orange color. The CV measurements show that the first oxidation peak is at 0.98 V and the second oxidation peak is at 1.41 V. The first oxidation peak can be attributed to the oxidation of the triphenylamine unit, and the second oxidation peak can be attributed to the oxidation of the π -backbone. The experimental HOMO and LUMO levels are 0.93 and -0.72 V, respectively, with a bandgap of 1.65 eV. It is important to note that the LUMO level lies above the TiO₂ CB, and the HOMO level is aligned well with the electrolyte. These ensure effective electron injection and reproduction of dye. The electron density distribution is predicted using density functional theory. The result shows that the HOMO levels are delocalized on the triphenylamine and thiophene groups of the π -conjugated bridge. The LUMO levels are delocalized on the BTD-phenylvinylcyanoacetic unit. This result is essential to understand that the directional electron distribution helps in electron injection into TiO₂ and regeneration of dye by quicker reduction of the I⁻/I₃⁻ dye.

DSSC using the RK1 dye is fabricated using an acetonitrile electrolyte. The electrodes used in this case is a double-layer structure, firstly, mesoporous TiO₂ followed by a TiO₂ scatter layer. The N719-based DSSC is used as a reference in this case as well. The IV curves are recorded at a standard illumination of AM 1.5, 1 Sun illumination along with IPCE measurements. To determine the device's optimal performance, the thickness of the TiO₂ film is varied from 4 to 13 μ m. The scattering layer of TiO₂ varying from 3.5 to 4 μ m is deposited.

The concentration of the dye from 0.2 to 0.5 mM is varied and used along with a coad sorbent of chenodeoxycholic acid. Using chenodeoxycholic acid improves dye loading characteristics and reduces the formation of dye aggregates on the TiO₂ surface. It is important to note here that, even at a low film thickness of TiO₂, the device's performance remains above 7% PCE. On further increasing the thickness of the TiO₂ film, the J_{sc} increases to 20.25 mA/cm² to produce a champion PCE of 10.2%. The performance of the RK1 and N719-based devices are nearly similar, with PCE values greater than 10% with similar dark currents. The photocurrent measurements from the IPCE spectra show that N719 performs relatively better than RK1 at longer wavelengths, whereas RK1 performs relatively better than N719 at shorter wavelengths. The transient photovoltage measurements are also analyzed. The charge extraction data for both the dyes are analyzed, and as expected, the RK1 dye shows a better response than N719. On calculating the electron lifetime constant, N719 dye showed a higher value than RK1. However, we can confirm with previous literature that such a phenomenon is very much observed in organic sensitizers. The lower V_{oc} value for RK1-based devices can be related to the lower-lying TiO₂ CB and reduced electron lifetime constant.

To measure the long-term stability of the device, volatile solvents like acetonitrile cannot be used. Hence, in this case, a solvent-free ionic liquid electrolyte is used for thermal stress and long-term stability studies of RK1-based devices. Two different electrodes are used: firstly, a standard



mesoporous TiO₂ electrode and a TiO₂ paste, which improve light-harvesting efficiency. With an 8 μm thick TiO₂ film and a 3.5 μm thick reflecting layer, the resultant photovoltaic performance is a J_{sc} of 15.40 mA/cm², V_{oc} of 0.665 V, FF of 69% and PCE of 7.36%. The light-soaking test is conducted under a light intensity of 1000 W/m² at 65 °C. On conducting the test, the PCE significantly increases. This phenomenon can be related to the increased penetration of the electrolyte and electrode activation. However, after 2200 hours, the PCE shows a notable linear degradation in PCE. After the devices are analyzed for 5000 hours, they retain nearly 75% of their initial PCE.

Through this work, we understood the usage of a simple sensitizer with an uncomplicated synthesis process, and low-cost precursors were capable of producing highly efficient devices using a novel approach. Moreover, the fabricated devices displayed enhanced stability even after 5000 hours with a slight loss in PCE, which paves the way for a future stable, inexpensive and efficient device.

Molecular photosensitizer with 1.24 V as V_{oc}

The notable advantages that DSSCs offer over other solar technologies are the capability to produce light-harvesting properties through both faces of the solar cell, aesthetic appearance, and inexpensive fabrication and synthesis procedures. Moreover, the same benefits of these devices have led to small- or large-scale implementations like the SwissTech Convention Center and the Science Tower of Graz. An alternative way to boost a photovoltaic device's performance is to improve its V_{oc} significantly. It has been shown that organic dyes, when paired with Cu(II/I) electrolytes, exceed a V_{oc} of 1.0 V. These values are comparatively higher when analyzed to the Cobalt or Iodine-based electrolytes. Dan Zhang and coworkers developed two dyes using this approach, referred to as MS4 and MS5. The MS4 dye uses a donor unit of N-(2',4'-bis(dodecyloxy)-[1,1'-biphenyl]-4-yl)-2',4'-bis(dodecyloxy)-N-phenyl-[1,1'-biphenyl]-4-amine and acceptor of 4-(benzo[c][1,2,5]thiadiazol-4-yl) benzoic acid (BTBA). MS5 uses a similar arrangement [8]. However, in the case of the donor atom, on increasing from n-hexyloxy to n-dodecyloxy, the MS5 dye is generated. The performance and properties of the dyes are compared with a reference dye NT35 that has the same donor unit as MS4, but the acceptor unit is cyanoacrylic acid (CA).

The UV-Vis absorption spectra for the dyes are recorded on a 2.2 μm thick TiO₂ electrode. MS4 shows a red shift by 46 nm compared to NT35, with a maximum absorption wavelength of 468 nm. The MS5 sensitizer also shows a similar absorption spectrum to MS4. The molar extinction coefficient of NT35 in the 400-500 nm range is nearly 5 and 3 times larger than MS4 and MS5 dye, respectively. However, the maximum absorbance of NT35 on TiO₂ is only 1.5 times larger. This indicates that NT35 has a very loose molecular packing on TiO₂. The dye loading amounts on TiO₂ are measured to be 2.6 x 10⁻⁹, 5.3 x 10⁻⁹ and 6.9 x 10⁻⁹ mol cm⁻² μm⁻¹ for NT35, MS4 and MS5 dyes, respectively. On conducting the CV tests, the E_{ox} results show 1.21, 1.17 and 1.18 V on TiO₂ for NT35, MS4 and MS5 sensitizers, respectively. Analyzing the values, having a more positive value than NT35 shows the suitable capability for dye regeneration. The zero-zero transition energies (E₀₋₀) on TiO₂ film are 2.48, 2.29 and 2.28 eV for NT35, MS4 and MS5, respectively. We can conclude that having a BTBA acceptor unit further reduces the energy gap for both MS4 and MS5. The E_{red} values show a value of -1.27, -1.12 and 1.10 V for NT35, MS4 and MS5, respectively. Similarly, having more negative values facilitates suitable electron injection from the sensitizer to the TiO₂ CB.



The devices fabricated used three sensitizers, particularly as $[\text{Cu}^{(\text{II})}(\text{tmby})_2]$ coupled with TFSI, LiTFSI and NMB in acetonitrile. The IPCE is determined for each of the device sensitizer equivalents. MS4 and MS5 have a near 50 nm red shift compared to NT35. The maximum IPCE value shown by MS4 and MS5 is nearly 82% at 510 nm, which is superior to NT35, having 75% at 400 nm. The energy offset levels between the dye/electrolyte and dye/ TiO_2 interface provide a method for proper dye regeneration and electron injection. The higher IPCE value also indicates the improved charge collection efficiency. Moreover, the transient photovoltage measurements show that MS4 and MS5 devices have longer carrier lifetimes than NT35. The NT35-based device showed a photovoltaic performance: V_{oc} of 0.95 V, J_{sc} of 5.96 mA/cm^2 , FF of 0.791 and PCE of 4.5%. The MS4-based device showed a performance of V_{oc} of 1.17 V, J_{sc} of 8.86 mA/cm^2 , FF of 0.73 and PCE of 7.6%. The MS5-based device showed a performance of V_{oc} of 1.24 V, J_{sc} of 8.87 mA/cm^2 , FF of 0.73 and PCE of 8%. The maximum voltage obtained using a $[\text{Cu}^{(\text{II})}(\text{tmby})_2][\text{TFSI}]_{2/1}$ electrolyte is 1.37 V. The V_{oc} difference between the NS5-based device and the maximum voltage recorded can be accounted for by the recombination effect taking place. On calculating the ideality factors, the MS5-DSSC showed the lowest value of 1.08 than MS4 and NT35. This indicates the reduced recombination that MS5 depicts and its reduced trap states. On conducting transient photovoltage decay measurements, an indefinite number of charges are being withdrawn from the TiO_2 film after a certain photovoltage, indicating that dye changes do not necessarily impact the conduction band and trap states. MS4 has twice the magnitude of its NT35 counterpart, whereas MS5 has a three times manifold. The dye loading is more profound in the MS4 and MS5-based devices, implying reduced charge recombination.

The co-sensitized dye used in this case is a dye referred to as XY1b for its superior spectral response along with MS5. The absorption spectra of MS5 and XY1b complement each other, enabling the device to have a broad spectral response. The IPCE spectrum of the XY1b and MS5 devices is higher than its counterparts. An XY1b-based DSSC produced a photovoltaic performance of, V_{oc} of 1.01 V, J_{sc} of 15.26 mA/cm^2 , FF of 0.763 and PCE of 11.8%. The co-sensitized device produced higher values with a V_{oc} of 1.05 V, J_{sc} of 15.84 mA/cm^2 , FF of 0.813 and PCE of 13.5%. Moreover, on conducting a light soaking test to evaluate the stability of the device, it retained nearly 93% of its initial PCE after 1000 hours of soaking at 45 °C.

The J_{sc} loss of the co-sensitized device is only 6% which is lesser than half of the XY1b-counterpart. This reduced J_{sc} loss can be attributed to the improved absorption spectral response and higher IPCE values. The DSSCs anchored on TiO_2 , and the electrolyte of LiTFSI and NMB in acetonitrile show a time constant (from TiO_2 to D^+) value of 49 and 61 μs for XY1b and the co-sensitized device, respectively. The regeneration lifetime of the D^+ with the electrolyte is found to be 5.7 and 6.0 μs , respectively, for XY1b and XY1b + MS5. The regeneration efficiencies are 86.4% and 91.0% for XY1b and the co-sensitized device, respectively.

The improved dye regeneration ability is partly responsible for the lower J_{sc} losses and high IPCE values. The V_{oc} losses are 26.0% and 23.7% for XY1b and co-sensitized devices. This result indicates how the latter device possesses reduced charge recombination in bulk and the device's interface. The dye loading amount for the co-sensitized part is $2.70 \times 10^{-8} \text{ mol cm}^{-2} \mu\text{m}^{-1}$, which is significantly higher than the individual counterparts, thus, retarding the recombination effect. The ideality factor for the co-sensitized device is also lower (1.27) than XY1b (1.41) and MS5, respectively. The FF_{TL} loss is also significantly lower (4.8%) than the XY1b counterpart (6.4%), further reducing the recombination effect. The FF losses are also calculated and found to be 9.4% and 5.8% for XY1b and the co-sensitized device, respectively.



The co-sensitized device shows how reduced charge recombination can impact performance and how a low ideality factor can influence a device's charge transporting properties. The co-sensitized device with an active area of 2.8 cm² was made and tested under an Osram 930 Warm White Fluorescent Tube to investigate the device's optimum performance further. The experimental energy gap was calculated to be 1.73 eV, giving a *PCE* of 49%, 51%, 54% and 57% under a light intensity of 100, 1000, 10000 and 314, 465 lux, respectively. The device is fabricated with a reduced concentration of Cu (II) electrolyte, as studies have shown how a reduced amount of Cu (II) electrolyte can minimize charge recombination to improve further V_{oc} and performance of the device, particularly under ambient light. A similar principle can also be used in the case of Cu (I). The device's performance is recorded at 1000, 500 and 200 lux. At 1000 lux, the device performs remarkably, with a V_{oc} of 0.98 V, J_{sc} of 138.2 $\mu\text{A}/\text{cm}^2$, *FF* of 0.815%, *PCE* of 34.5% and a P_{max} 109.8 $\mu\text{W}/\text{cm}^2$. A considerably high *PCE* value was also obtained for higher device areas, 31% and 26% at 1000 lux for 8 and 20.25 cm², respectively. It is essential to highlight that the devices also performed significantly well under 200 and 500 lux with a V_{oc} above 0.92 V, *PCE* between 32-33% and an ideality factor of 1.25. The *PCE* levels obtained from this particular configuration and engineering are surprising and a feat because such levels even exceed many of the current PSCs, Si-based solar cells, CIGS, and GaAs solar cells.

This study analysed how molecular engineering and careful usage of donor and acceptor units can suitably tailor the *PCE* levels for Cu-based DSSCs. Moreover, the improved *PCE* levels can be attributed to the reduced ideality factor and minimal charge recombination effect. The impact of photovoltaic performance can also be related to the influence of Cu-redox electrolyte on the device.

MoSe₂/Mo counter electrodes for efficient DSSCs

For traditional DSSCs, the counter electrode (CE) used is Pt. However, it is essential to note that as commercialization of these devices occurs, we need to choose cheaper and more viable materials that reduce the cost of the device. Several possible candidates have been considered previously, like metal oxides, sulfides, nitrides, and carbon-based materials. Selenides have been studied extensively for their interesting optoelectronic properties previously used in solar cells and photocatalysis. However, the series resistance of these devices (R_s) is exceptionally high, leading to reduced *FF* and performance. This can be related to the poor contact between the CE and substrate. In this section, Haijie Chen and coworkers designed a bilayer CE structure using MoSe₂/Mo [9]. The top MoSe₂ layer acts like the I₃⁻ reduction site, and the bottom Mo layer acts as the charge collector for extracted charges.

The preparation method is a Mo thin film on the substrate. The electrical conductivity of the Mo film is exceptionally high, with a value of 28.1 $\mu\Omega$ cm. The Mo-based glass is annealed in an atmosphere of Se to form a bilayer of MoSe₂/Mo at 500 °C for 30 mins. The resultant surface is found to be homogeneous with a smooth morphology. On conducting an XRD analysis, the Mo peaks are present, which shows the presence of Mo in the bilayer configuration. The cross-sectional SEM measurements show a bilayer structure with a 770 nm thick Mo layer and 558 nm thick MoSe₂ layer. On doing an EDS line scan result, Se was not in the bottom layer, whereas the upper layer showed a liner distribution of Se across the Mo surface, indicating good contact between the 2 layers. The Fermi level of MoSe₂ and Mo are nearly equal, and if the energy band of MoSe₂ upsweeps, a high conductive region is formed, which facilitates charge transfer.



On fabricating a device with the architecture of MoSe₂/Mo CE, the J_{sc} obtained is 15.07 mA/cm², V_{oc} of 0.805 V, FF of 0.67 and PCE of 8.13%. The obtained photovoltaic performance is comparable with Pt-based CE with a J_{sc} of 16.11 mA/cm², V_{oc} of 0.794 V, FF of 0.63 and PCE of 8.06%. It is essential to understand that a thin layer of MoSe₂ is insufficient to reduce I₃⁻ whereas a thick MoSe₂ layer creates a lot of series resistance and is not suitable for charge transfer. Thus, it is vital to understand the optimum layer of MoSe₂, which is found to be 558 nm. The CV measurements are taken, and the Pt and Mo-based CE have two pairs of redox and cathodic peaks that correspond to the two-step reduction process of I₃⁻.

The MoSe₂/Mo CE has a higher charge/current density, improving charge transport, making it a plausible candidate for CE to replace Pt. The EIS measurements of both the CEs are taken. There are 2 semi-circles formed at low and high-frequency regions, respectively. The high-frequency semi-circle is related to the Iodine reduction and its charge transfer resistance. The semi-circle in the low-frequency region is related to the series resistance. Here R_s is attributed to electron collection from an external circuit. The R_s value for the Mo-based electrode is 2.64 Ω, whereas for the Pt-based electrode is found to be 15.98 Ω. The R_{ct} is related to the charge transfer resistance between the electrolyte/CE interface. The R_{ct} values are 0.30 Ω for MoSe₂/Mo and 8.95 Ω for Pt.

This study showed how MoSe₂/Mo CE could be prepared by an in-situ process using a bilayer structure. Moreover, the analysis showed how CV, EIS and photovoltaic performance for Mo-based CE improved the device compared to Pt, which is much more superior. This configuration was also reflected on a bifacial CIGSSe solar cell. Compared to previous lectures, the obtained R_s and R_{ct} values, in this case, are much lesser than the reported values, making it an even more beneficial candidate for CEs.

Hot-bubbling SnO₂ with TiO₂ for efficient DSSCs

A DSSC with TiO₂ photoelectrodes have suffered from low electron mobility, sluggish responses and, in some cases, increased charge recombination. Materials like Nb₂O₅, ZnO, SnO₂ and bi-functional materials have been explored as suitable alternatives. In particular, SnO₂ has grabbed much attention because of its high electron mobility and larger bandgap with a more minimum value of CB minimum than TiO₂, facilitating suitable electron injection and transfer. However, the lower V_{oc} values of SnO₂-based devices can be attributed to the recombination process and position of the CB. In this section, we shall explore the works of Xiaoli Mao and coworkers, who developed a high crystalline phase of SnO₂ which can reduce recombination and align the energy band suitably [10]. This was possible through a method called hot-bubbling synthesis, through which the size of the SnO₂ crystals could be controlled, and desired sizes could be obtained. Homogeneous nucleation rates and sites were observed because of the gases' high-temperature processing and fast diffusion rate.

The hot-bubbled SnO₂ formed was highly crystalline in nature through this fabrication method. After a prolonged growth time, the SnO₂ clusters did not grow. This indicates that SnO₂ has a high-energy barrier in hot OA-ODE-OLA solutions. The XRD analysis shows the presence of a tetragonal SnO₂ molecule. The XRD results show multiple patterns, where the strong patterns can be associated with TiO₂, whereas the weaker patterns can be associated to the TEM results depict semi-spherical SnO₂ particles with diameter ranges from 3.0-4.0 nm. Under HRTEM, lattice fringes were observed, showing the high crystallinity of SnO₂. The fringe distances were found to be 0.142 and 0.330 nm. The TEM results show how SnO₂ is well-dispersed in the composite film,

and the HRTEM results show the close and well-formed packing between SnO₂ and TiO₂. Comparing this to the traditional method of synthesizing SnO₂ through a hydrothermal method, the average diameter is 20 nm. This sample is referred to as S₂₀.

It was not possible to use SnO₂ entirely as a photoelectrode. Instead, this was mixed with commercial TiO₂ composites in different ratios. The ratios vary from 0 to ∞. The porous nature of all the anodes is visible. However, the S7.5 showed the most excellent porosity distributed across the film homogeneously. The mixed particle size of SnO₂ and TiO₂ forms a cohesive valuable network for a photoanode.

These analyses depict the compatibility between SnO₂ and TiO₂. The FT-IR spectra show the broad absorption range of SnO₂/TiO₂ composites in 400-800 cm⁻¹, related to the Ti-O-Ti bonds. The maximum at 1063 cm⁻¹ in S7.5 and S12.5 can be related to the Sn-O-Sn bonds. The highest absorption is seen in S12.5, which can be related to the uniform distribution of SnO₂ in TiO₂.

The N₂ absorption-desorption spectra isotherms of varying SnO₂/TiO₂ composite films can be studied in Table 3.

Table 3. N₂ absorption-desorption results of the composite films [10]

| Film Type | Dye Loading (10 ⁻⁷ mol cm ⁻²) | Surface Area (m ² g ⁻¹) | Pore Volume (cm ³ g ⁻¹) | Pore Size (nm) |
|-----------|---|---|---|----------------|
| S0 | 1.70 | 45.4 | 0.22 | 28.4 |
| S7.5 | 1.90 | 53.0 | 0.27 | 20.5 |
| S12.5 | 1.57 | 53.6 | 0.25 | 18.7 |
| S∞ | 0.71 | 64.8 | 0.06 | 3.9 |

From the N₂ absorption-desorption results, we can see that, on incorporating SnO₂ in small amounts to TiO₂, the surface area increases, a valuable property for photoelectrodes. The improved dye loading ability can also be noticed when adding SnO₂ to TiO₂. The UV-Vis absorption spectra of the samples are recorded. S7.5 shows the highest range of absorption spectra with a considerably higher dye loading than the rest of the film types. The loading can be related to the pore volume and surface area, and thus, adding SnO₂ to composite TiO₂ can increase N719 loading. However, increasing the SnO₂ amount past a specific optimum value, the pores are sealed, and dye loading decreases. Using a mixture of TiO₂ and SnO₂ decreases the interfacial resistance of the device. As a result, the charge mobility of the device increases. On adding SnO₂, the charge incorporation increases a lot, and in the case of S7.5, the effect between SnO₂ and TiO₂ compliment each other the most, which improves charge transfer. In this case, the addition of SnO₂ shifted the CB minimum in a favorable manner which genuinely makes this feature an additive for improved IPCE and photoelectrodes.

On recording the photovoltaic parameters, the addition of SnO₂ reduced the V_{oc} value from 0.82 to 0.79 V. However; the J_{sc} value increased significantly from 8.2 to 15.4 mA/cm². The PCE value was 6.7% (S7.5) higher than a modification done by Cao et al., TiO₂ coated with SnO₂ hollow microspheres. The EIS measurements show double semicircles in small and high-frequency ranges. The R_s values vary from 10.8 to 22.3 Ω m². The S7.5 has a lower value for R_s which indicates the improved ohmic contact of the photoanode. A smaller value for R_{ct} (Charge Transfer Resistance) was also obtained for S7.5 (25.3 Ω cm²). However, the R₁ values are nearly equal. The reduced R_{ct} values can be attributed to the faster charge transfer and mobility from the



electrolyte to the photoelectrode. It is essential to note that, on adding SnO₂ to TiO₂, there is a notable increase in surface area, which possibly improved the photovoltaic performance. However, on adding more SnO₂, the photovoltaic performance begins to decrease, indicating an optimum ratio for SnO₂ and TiO₂ for improved performance. The electron transport and recombination phenomenon at the interface are studied through IMVS and IMPs. The electron transport time (T_d) is 3.99, 1.26, 1.12, 1 and 317.47 ms for S0, S5, S7.5, S12.5 and S ∞ films. These values were highly reduced when compared to a pure TiO₂ commercial photoelectrode.

Moreover, the recombination time constant (T_r) is increased, indicating the reduced recombination in the case of SnO₂/TiO₂-based photoelectrodes. The charge collection efficiency (η_{cc}) was calculated, and the highest efficiency value recorded was 99.7%. Hence, this analysis shows that incorporating SnO₂ reduced charge recombination and improved electron transport and mobility. The reduction in V_{oc} value is not yet known, but possible reasoning can be developed with further evidence.

Through this work, the modification of SnO₂ with TiO₂ produced a photoanode with suitable energy band alignments, reduction in trap sites, provides more charge transfer pathways, improved electron transfer and mobility, more excellent conductivity, and higher electron diffusion lengths, which can be reflected through the photon-to-electron conversion efficiency.

Co-polymer gel electrode for a high-efficiency DSSCs

Commercialization of DSSCs requires the usage of suitable electrolytes and solvents such as acetonitrile and 3-methoxypropionitrile (MPN). However, these solvents possess issues like volatility and fluidity, which can impact the long-term performance of the device. Recently, gel-based electrolytes have been incorporated into devices, and the performances obtained are comparable to their liquid electrolyte counterparts. Amongst the gel-based electrolytes, polymer gel electrolytes follow a simple preparation method and have an excellent liquid trapping capability. Chen et al. reported the usage of in-situ gelation of PAN-VA and acetonitrile-based electrolyte with an efficiency of 9.5% using a TiO₂ nanofiller. Other than the I⁻/I₃⁻ redox couple, the cobalt (II)/(III) redox couple are non-corrosive and do not depict any visible region light absorption properties.

In this section, Wanchun Xiang and coworkers used a cobalt gel electrolyte with a varying amount of (4-10%) PVDF-HFP in acetonitrile. The influence of a polymer-based gel electrolyte is analyzed, and the photovoltaic performance is studied [11].

The rheology results show that even a 4wt% of PVDF-HFP produces a gel matrix. The gelation time required is dependent on the polymer content. It varied from 5h for 4wt% to 30 min for 10 wt%. The devices fabricated used a 6 μ m thick TiO₂ electrode. The devices used an MK2 dye, and on using 4wt% of the polymer, a PCE of 8.7% is measured. It is important to note that this recorded PCE is the highest value noted for a Co-based redox couple. The J_{sc} , V_{oc} and FF values are 884 mV, 13.9 mA/cm² and 0.71, respectively, under 1 Sun illumination. These values were compared with a liquid-based electrolyte. Compared to such an analysis, the J_{sc} obtained was comparatively lower, and the V_{oc} remained nearly the same. The photovoltaic performance is also recorded at 0.1 Sun illumination. The performance, in this case, was 10%, and this value did not vary even for 10wt% of polymer. This indicates a constant and high-power yield using innovative technology. This is the highest value recorded for any solid-state DSSCs at 0.1 Sun illumination. The IPCE results show a high conversion efficiency with a constant plateau at 75% in the range



of 400-600 nm showing the appropriate and suitable light-absorbing properties. The viscosity of the electrolyte greatly influences the diffusion of charge carriers in the device. The viscosity is studied by calculating the electrolyte's apparent diffusion coefficient (D_{app}). A small limiting current is produced at lower concentrations on varying the Co(II)/(III) ratio. This indicated that the diffusion-determining species is solely the redox couple. On conducting a comparative analysis, the liquid electrolyte shows a higher D_{app} value when compared to the polymer electrolyte counterpart, reducing up to 50% when 10wt% polymer is added. Thus, these results show that the diffusion rate significantly decreases when adding a certain amount of polymer to the electrolyte.

The transient photocurrent measurements are studied and analyzed. At the low intensity of light, a steady photocurrent value is obtained, slightly delayed under the absence of PVDF-HFP. As the PVDF-HFP content increases, the current spike increases, and the photocurrent gradually decreases. This shows the reduced charge transportation in the polymer-based electrolyte giving rise to a reduced photocurrent. The charge transfer resistances at the TiO_2 /electrolyte interfaces, electron lifetime and measured V_{oc} values are identical despite varying the polymer content. The chemical capacitance distributions show a similar state density and minor change in TiO_2 energy bands.

The stability of the devices is studied with and without the 4wt% polymer content. The fabricated devices are placed under continuous 1 Sun illumination. After nearly 700 h, the device with the polymer retained 90% of its initial PCE , whereas the polymer-free device retained 90% of its initial PCE after only 200 h, which further dropped by 75% after 500 h. The primary reason for a drop in J_{sc} for photovoltaic performance can be attributed to the solvent's partial evaporation, which reduced surface contact area and increased viscosity.

This study produced a device with a PCE of 8.7%, which even increased to 10% under 0.1 sun illumination using a Co-gel electrolyte. The device's charge carrier transport and interfacial characteristics can be further improved to get a superior value of PCE and improve the diffusion of redox species.

Strategies to improve DSSC performance

The Shockley-Queisser limit of a DSSC is 33.8% under AM 1.5 G and 1000 W/m^2 irradiation. The optimal bandgap through this limit is 1.3 eV which is reduced to 1.9 eV and a PCE of 25%, which is the theoretical value. The J_{sc} value at this condition is 17 mA/cm^2 . The V_{oc} value is equal to E_g/e . Here the bandgap is determined by the E_c level of TiO_2 and the redox potential of the electrolyte. This value obtained is always lesser than the bandgap of the dye.

Additives, chemical modification, and thin metal oxides can alter the set level. These added layers/modifications can improve the DSSC performance by altering the charge transfer kinetics. It is important to note that even redox electrolytes play a crucial role in increasing the redox potential [12]. Some electrolytes might aid recombination, which may correspondingly impact the Fermi level. The best V_{oc} value obtained for a TiO_2 -based dye is 1.4 V, for a $Co(bpy)_3$ is 0.9 V and for a device using Spiro-OMeTAD is 0.8 V. It is important to have a long electron lifetime to increase the V_{oc} of the device. The electron transport time should be lesser than the lifetime to get maximum output. The transport resistance decreases when a $TiO_2/C(TiO_2)$ is charged. The R_{rec} value should be as high as possible to increase current collection efficiency and output voltage. As the thickness of a particular layer increases, the R_{rec} value decreases. R_s values are



nearly impossible to eradicate. Han et Al. showed that it was possible to reduce the R_s value to $1.8 \Omega/\text{cm}^2$ by modifying the catalytic performance of the counter electrode. The unavoidable resistances cannot be minimized. However, the use of PEDOT at the counter electrode has been shown to resist short-circuiting.

The usage of Co-based redox electrolytes along with porous mesoporous films is usually better for device performance. Moreover, the addition of an anti-reflective layer on TiO_2 has been shown to improve light-harvesting efficiency. Changing the mesoporous film by having reflective particles or voids is also possible. The TiO_2 used is known for being an excellent photocatalyst. However, the high bandgap of TiO_2 is unfavourable, and this can be altered by using a thin layer of Al_2O_3 or MgO . Recently, even SnO_2 has been a helpful candidate in DSSCs, with only electron mobility being its only limitation, thus, having lower performances than TiO_2 [12].

A photosensitizer used in a DSSC should have a robust structure with valuable properties to prevent charge recombination and encourage electron and hole transfer. Apart from this, an efficient dye has a high excited lifetime and yield. As excited lifetime increases, the injection efficiency increases. Wang et Al. used an R6 dye on a mesoporous Al_2O_3 film to generate enhanced device efficiencies. Co-sensitization is also a viable approach to generating higher performance. A higher loading can also improve the output current of the DSSC device.

A perfect dye should have the following properties [13]:

- Absorbance near IR and visible region
- Strong anchoring group for binding to the photoanode surface
- HOMO and LUMO levels should be well aligned with the electrolyte and photoanode
- Fluorescent properties
- Hydrophobic
- No aggregation
- Solid thermal, mechanical, chemical and electrochemical stability

Ru-based dyes' strong photoelectrochemical properties have made it a staple material in DSSCs and a first of its kind to record high efficiencies. Alternatives like Fe, Pt, Cu, Rh and Os-based dyes are being investigated. Organic dyes are also another option because they are eco-friendly and have higher extinction coefficients. Moreover, its tunable energy levels can improve the absorption regions of the device. Studies have shown that steric hindrance decreases the dye loading on the photoanode surface, reducing the short circuit current value. Crown ether substituted carbazole dye with TiO_2 photoanode and iodide/triiodide electrolyte produced an efficient device because the Li-ions coordinated with the crown ether prevented the unnecessary migration of TiO_2 . A photosensitizer with an oligothiophene-substituted unit produces an efficiency close to the traditional N719-based devices. On comparing the performance, the triphenylamine device produces the highest V_{oc} due to the blocking effect of phenyl groups. The coumarin device has the lowest V_{oc} , but the high absorption coefficient yields a higher J_{sc} , compensating for the PCE value. Squaraine-triarylamine conjugate dyes with an additional number of anchor groups improve the device's efficiency.

Researchers concluded that having a multichromophoric structure with one chromophore having light-harvesting properties and possessing the acceptor molecule is a strategy to improve the device's efficiency. Studying the optimum number of alkyl groups to positively impact the performance of a DSSC is of utmost importance. It was studied that the optimal number is 3 to 4



thiophene units in hexyl substituted oligothiophenes. Porphyrins and phthalocyanines are other groups of dyes that can be used in their individual or metal complex forms. The organic part of this dye improves the photoelectrochemical and light-harvesting properties of the device. Phthalocyanines with different modifications were studied. In a particular modification, varying the phthalocyanine cycle parallel to the TiO₂ surface reduces recombination but produces a counter effect of reducing the device efficiency. Bulky substituents could carry out the same effect but at moderate efficiency. A device with Zn-porphyrin complex and a [Co(bpy)₃]^{2+/3+} resulted in an efficiency of 7.8%. Devices using porphyrins as a dye have attained efficiencies nearing Ru-based devices.

Moreover, unlike Ruthenium dyes, porphyrins can be tuned to vary the HOMO and LUMO levels. Moreover, further research can be done to reduce dye aggregation, improve absorption properties and enhance the long-term stability of the molecule. A porphyrin dye is a practical solution for a porphyrin GY50 dye with di(p-alkylphenyl) amine in the meso-position and a benzothiadiazophenyl spacer between the porphyrin cycle and carboxyl group [14].

An ideal electrolyte should possess the following properties [13]:

- Effective regeneration of the dye
- Fast diffusion of charge carriers, high conductivity and effective contact
- Long term thermal, chemical and thermochemical stability
- Not be corrosive
- It should be transparent to absorption regions of the dye

Apart from the regular iodide/triiodide system of redox mediators, Cobalt redox mediators have been highly recommended. The wide range of potentials, solubility in different solvents and their unique chemical structure gives these compounds an upper hand. Water-based electrolytes have exhibited more excellent stability, which paves the way for eco-friendly devices. However, the slow electron transfer of Co-based redox mediators is what restricts them from commercialization. Using additives like triphenylamine (TPA) helps overcome such limitations, producing faster electron transfer and higher V_{oc} values. Although Cu-based redox mediators show faster recombination rates, the electron lifetimes are surprisingly long, which can be further developed to obtain favourable performances. The usage of a mixture of ethylene carbonate and acetonitrile and tetrapropylammonium iodide and iodine is a suitable dye for high efficiency, but it impacts the performance of TiO₂ negatively in the long run. Redox pairs like Br/Br₂, SCN⁻/(SCN)₂, and Co^{II}/Co^{III} are being heavily researched, but their performance is not comparable to that of the I⁻/I₃ pair. Another approach to improve electrolytes is using additives. In this case, the most common additive is guanidine thiocyanate, which modulates the electrolyte band levels and reduces the recombination rate.

Liquid ionic electrolytes are also of notable importance. They are stable and have high conductivity and low vapour pressure at room temperature. However, the property of them being able to evaporate or leakage restricts their usage in practical implementation. Creating gel and solid-based electrolytes is being considered as an alternative. Lithium iodide and 3-hydroxypropionitrile are solid electrolytes used in a DSSC device. Unfortunately, it possessed low conductivity and poor photoanode surface contact, which was resolved partially with SiO₂. Polymer electrolytes are also being considered. For example, the polyethylene oxide and polydimethylsiloxane mixture were one such case, but they yielded low *PCE* values. Egg albumin was also studied as a possibility for gel electrolytes. The protein was initially functionalized to



improve cross-linking and conductivity. ZnAl double-layered hydroxides were also used as additives, whereby a notable increase in V_{oc} values was observed [13].

The structure of the semiconductor used plays a crucial role in device performance. The use of TiO_2 nanofibres improves the efficiency to nearly double the value compared to TiO_2 nanoparticles. TiO_2 modified with graphene oxide, and nitrogen-reduced graphene oxide produced an efficiency of 7.19% with an optimal loading of 0.2 wt% of nitrogen-reduced graphene oxide. ZnO is also considered a suitable alternative because of its high electron mobility. However, when compared to TiO_2 , ZnO has shallow stability. On loading a similar amount of ZnO and TiO_2 on a particular device, the TiO_2 counterpart showed nearly 4 times the value of the ZnO-based device. Other alternatives like SnO_2 , Nb_2O_5 and NiO are being studied, but much research is pending to commercialize these materials.

The carboxyl group is the most widely used anchoring group. However, techniques have been used that do not require an anchoring group [12]. Hafnium, Zirconium porphyrin, and phthalocyanines have been synthesized with a high affinity for polyoxometalates, forming a solid binding phenomenon, thus eliminating anchoring groups. Similarly, carboxyl-based ligands with a nitrogen-containing heterocycle bind to the photoanode surface to form a metal complex.

Co-adsorbents are used to prevent recombination and dye aggregation on the photoanode surface. Cholic acid derivatives are often used as co-adsorbents. A DSSC using thiophene substituted bithiazole resulted in an efficiency of 1.13%. On incorporating it with CDCA, the dye efficiency increased by 1.25%. A new co-adsorbent based on triazoloisoquinoline was synthesized. This was coupled with N719 dye to increase the efficiency from 8.36 to 8.83%. It is essential to understand that the optimal amount of co-adsorbent being used is also necessary.

Co-sensitizing various dyes together is a valuable strategy for improving the device's output current, voltage and electron lifetime. However, it is essential to note that the electron lifetime values from each dye are similar. A useful co-sensitizer for N719 is $[Cd_3(IBA)_3(Cl)_2(HCOO)(H_2O)]_n$ and $\{[Cd_{1.5}(IBA)_3(H_2O)_6] \cdot 3.5H_2O\}_n$. A co-sensitized device with Zn-phthalocyanine complex and triarylamine-bithiophene dye was formed to increase the device's efficiency with a value greater than its counterparts [13].

In the case of solid-state DSSCs (ssDSSCs), the usage of a definite HTM is the only differentiating factor. Materials like PEDOT:PSS and Spiro-OMeTAD are the common ones used. However, the compatibility of these materials with a mesoporous film. The faster recombination rates of ssDSSCs are also a significant issue that needs to be solved, further limiting the output voltage values. A study was conducted where a dried ssDSSC using a Cu-redox electrolyte performed exceptionally well, regarded as a zombie solar cell. Pyrrolidinium ionic crystals have been regarded for forming a 3-dimensional matrix responsible for the device's high efficiency and stability.

High-performance DSSCs are of profound interest because of their unique photovoltaic properties, which can be harnessed for multiple applications. However, several issues need to be solved and addressed to top a traditional solar cell. The practical usage of the DSSCs comes to enhancing the device's performance in large areas. In actual conditions, as the area of the device increases, the efficiency decreases. The long-term stability of the device needs to be looked into, thus calling the need for scaling-up and optimization [12, 13].



Commercialization of DSSCs

Ricoh is an electronics and technology-based company that aims at developing products and services to build more innovative solutions. Ricoh has developed a fabrication procedure capable of producing a standardized and regulated quality of ssDSSCs to ensure maximum efficiency. Today, Ricoh's 300 mm ssDSSC panel is one of the most used mass-produced samples. Ricoh believes that DSSCs being a high efficiency and high open-circuit voltage device, can undoubtedly be used to charge secondary cells. The usage of DSSCs can be expanded to LEDs and switches where even under low illumination, the photovoltaic activity is not limited [15].

Exeger is a Swedish-based electronics company that works on products incorporating sustainable energy technologies. They have a patented technology that permits them to use DSSC commercially. Their innovation is termed Powerfoyle, which has been actively used in their products. For example, the Exeger headphones are coated with a DSSC where the device with 1 hour of illumination enables 3 hours of playtime which also works during a cloudy day to allow 2 hours of playtime [16].

G24 innovations created the first commercial application. Here the devices produced were thin, flexible and used in the case of portable electronics. The DSSCs are used for purposes like camping and powering LED systems. It uses a roll-to-roll manufacturing process. This allows the DSSC to appear in a metal foil, reducing labour efforts. G24i believes that its innovation can solve the problems experienced by batteries, and the incorporation of DSSCs in bags, and tents, can be used to charge electronic devices like mobile phones, cameras and portable systems. G24i have even large-scale purposes of DSSCs where their innovation has been used in advertising for both outdoor and indoor applications. They are currently working on adding this innovation to laptops, mobile phones, GPS systems, and AV devices to extend their lifetime and develop more commercial designs for their products [17].

The USA has been a pioneer in DSSC applications, where it has pioneered several innovations in various departments. The rising concern of depleting non-renewable sources of energy was realized rather quickly by the USA, where they shifted to renewable sources quickly, with DSSCs being a valid contender in this case. The application of DSSCs in the US market is segregated into a few categories: outdoor advertising, charging, embedded electronics and automobiles. As of 2019, 33.3% of DSSC applications were used in portable charging because of their high power output and fast recharging rates. Building-integrated photovoltaics is a field that DSSCs have captured massively (13%) as it is forecasted to power residential areas and domestic requirements. DSSCs are in line to revolutionize grid technology as it aims at decentralizing power requirements with dye-powered applications paving the way in the coming years. Automobile integrated photovoltaics is a massive market that DSSCs can capture, especially in regions like North America and Europe, to propel the automotive market further. Some notable companies in DSSC applications are 3G Solar, Sharp and Fujikura [18].

DSSCs Market Characterization

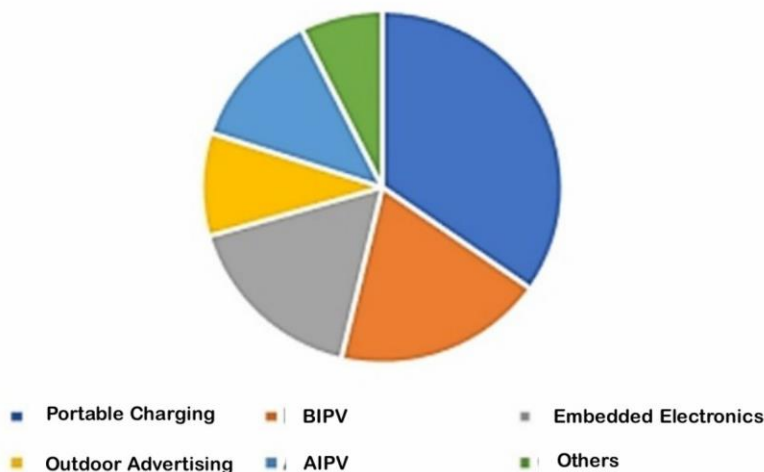


Figure 2. DSSCs Market Categories

3G Solar manufactures several DSSC-based products such as sports monitors, building sensors, portable medical devices, surveillance cameras and wireless products. The principle behind their commercial activities is very straightforward - optimizing existing DSSC technologies. They have merged aesthetics with functionality to create all its products with high power, low cost, coloured devices, high transparency and flexible characteristics. Moreover, unlike other solar technologies, 3G Solar's products provide a nearly constant efficiency [19]. Sharp has also developed a similar solution where it made the world's highest level of power generation for indoor applications with IoT principles. It provides an LCD with RE embedded controllers' continuous and constant operation with environment indoor lights. This can be used for indoor applications, IoT, and industrial equipment [20]. Fujikura's DSSC products are personalized as per the consumer's requirements. They have 2 variants: Indoor - credit card-sized, 4 cell modules, and Outdoor - passport-sized, 8 cell modules. The indoor and outdoor products can produce 1.5 V and 3.0 V, operating between -30 to 50 °C with a light intensity of up to 100,000 lux, respectively [21].

Research on fruits, vegetables and flowers

Flowers

Desalegn and coworkers conducted a study using natural dyes obtained from flowers, namely, *Amaranthus caudatus* (AC), *Bougainvillea spectabilis* (BS), *Delonix regia* (DR), *Nerium oleander* (NO) and *Spathodea campanulata* (SC) [22]. The flowers were initially collected in sufficient amounts. They were allowed to dry for 30 days after collection and then crushed into powder. The powders were then dissolved in different solvents like ethanol and HCl to extract the dyes.

AC and BS were dissolved in HCl and ethanol and mixed to create a hybrid dye. The dyes were then stored and covered with aluminium foils to prevent light degradation. The slurry obtained was then filtered to obtain a clear dye solution. The photoanode used in this case is TiO_2 . The ITO sheets used were made conductive using PEDOT:PSS, and a polymer gel electrolyte is used based on a PVP polymer.



The absorption characteristics of the dyes are studied. AC and BS extracted on ethanol produced absorption maxima peaks at 665 nm and 413 nm. The main component of these dyes is chlorophyll.

The HCl version of these dyes produced maxima of 500-600 nm for AC and 400-600 nm for BS. The mixed version of these dyes produced maxima at 670 and 536 nm for AC and 668, 536, 479, 446 and 416 nm for BS. For DR, there is an absorption peak at 516 nm, which corresponds to the anthocyanin's component in this dye. NO and SC in HCl did not have any notable absorption peaks in the visible region. This can be attributed to the fact that anthocyanin was the component extracted vigorously in HCl, which does not absorb light in the visible region. On acidifying this, it appeared to have a colour. This can be concluded that anthocyanin exists in an equilibrium relationship between quinoidal and flavium cation.

The photovoltaic performance of these dyes is recorded. The FF are above 50%, V_{oc} varies from 0.45 to 0.55 V, J_{sc} varies from 0.013 to 1.82 mA/cm². A V_{oc} value of 0.55 V and J_{sc} value of 1.82 mA/cm² were obtained for ethanol-extracted AC, with a PCE of 0.61%. This efficiency value obtained is one of the highest recorded for natural dyes and comparable to other studies conducted. The relatively high performance can be related to the broad absorption characteristics of the dye on TiO₂. Moreover, AC has the shortest skeleton distance between the dye and TiO₂ surface, which helps in electron injection.

BS has a much lower performance than AC when extracted by ethanol. This can be related to BS's higher chlorophyll concentration, leading to dye aggregation (concentration quenching). The performance of AC and BS extracted by HCl were also studied. The AC and BS efficiencies were 0.61% and 0.033% in ethanol and 0.325% and 0.018% in HCl, respectively. The efficiency for the mixed dye (0.114% for AC and 0.164% for BS) was lower than the sum of their counterparts. This indicates that AC and BS do not have complementary or synergistic effects that could contribute to optimizing the device. The reasons for such an occurrence are a) AC and BS absorb light from a similar region which can lead to optical losses or reduced exciton generation, and b) solid steric hindrance amongst the AC and BS dyes restricts uniform and regular packing on the TiO₂ surface, leading to limited electron transfer. The dyes extracted by ethanol had higher performances than their HCl counterparts. This is because anthocyanins extracted are much more soluble in ethanol than in HCl. Its higher solubility in ethanol reduces dye aggregation, which eventually contributes to higher efficiency.

DR extracted using HCl showed a PCE of 0.03%, SC with 0.003% and NR with 0.013%. In the case of DR, although the main component was anthocyanin, there were no carboxyl or hydroxyl groups present which could behave like anchoring groups to bind to TiO₂. The IPCE measurements show that AC had a maximum efficiency value of 52% at 430 nm with ethanol and 43.5% at 320 nm with HCl. BS shows a maximum efficiency of 27.7% at 410 nm with ethanol. The mixed dye and HCl peaks occur with 5.8% at 345 nm and 16.7% at 330 nm for BS dyes, respectively. DR shows a maximum efficiency of 5.1% at 340 nm. NO shows a maximum efficiency of 4.7% at 330 nm.

A significant blue shift was observed for AC, BS and DR dyes due to the interactions between the dye and TiO₂. Natural dyes like this should be considered even in the future because of the enormous scope for development, eco-friendly, low-cost and energy-efficient mechanisms.



Fruits and vegetables

M C Ung and coworkers conducted a study where they fabricated DSSCs using dyes obtained from fruits like Black Olive, Mangosteen and Wild Mangosteen. Along with this, the dye obtained from Blueberry is used as a standard reference. The study aims to understand the photovoltaic performance of anthocyanin dyes and the performance variation with a light source and counter electrode [23].

The dye sources were initially cut into small pieces, crushed, and washed with distilled water to obtain dye solutions. The samples were then crushed and mixed with distilled water to obtain a coloured dye solution. The solid residues were separated, and the remaining solution was used as the sensitizer. Even N719 dye was fabricated and used as a standard measure.

All the dyes show a broad spectral range from the UV-Vis absorption spectra, especially in the visible region. Thus, confirming that all the dyes are capable of becoming DSSC sensitizers. However, the absorption range and characteristics of each dye were very different. This can be related to the fact that different type and concentration of anthocyanin is present in the dye solution. It was observed that Black Olive showed the broadest and most broad absorption spectra.

All the dyes have light-harvesting and electron injection properties, making them slightly suitable for further device performance. Thus, making it possible to study the photocurrent and photovoltage measurements. However, studying all the dyes shows that Black Olive shows the highest efficiency because of its higher intensity and broad absorption properties. This also results in higher FF . The device measurements are as follows: $V_{oc} = 0.543$ V, $J_{sc} = 0.11$ mA/cm², $FF = 0.54$, $PCE = 0.08\%$.

The broad spectrum of sunlight enabled DSSCs to function efficiently. However, if this light source is varied to metal halide lamps that have a narrower spectrum, the performance of the DSSC correspondingly decreases. This can be related to the fact that, at broader spectral regions, more excitons or electron-hole pairs are generated, therefore, producing more current. This can be seen through the performance of Black Olive under a metal halide lamp, having 0.08% PCE but under sunlight, having a PCE of 0.13% .

A carbon-based counter electrode provides the DSSC with extra surface area with a porous morphology to facilitate electron transfer to the load and result in a higher available PCE . Carbon paste as a CE provided a higher PCE , FF , J_{sc} and V_{oc} value than Carbon soot. This can be attributed to better contact between Carbon paste and FTO, which is much more robust, with faster electron transfer.

This study shows that DSSCs using Black Olive can be considered a viable anthocyanin-based device. However, Black Olive can enhance performance with different light sources, counter electrodes, and materials; higher efficiencies can be worked.

Conclusions

DSSCs are one of the most promising and innovative photovoltaic devices out there that has the potential to become highly commercial. The examples reviewed in this article highlight how easy tuning and molecular engineering can produce impactful DSSCs. Each component of a DSSC plays a significant role in the device's performance and stability. It's very characteristic of low-

processing costs, abundant material sources, and easy fabrication process create a substantial advantage for this innovation to stand in the market. Comprehending the potential of DSSCs, the various materials that can be used, strategies to adopt for high-efficiency DSSCs, advantages and disadvantages, commercial activities, research undergoing in India and the novel fruits and flowers that are being studied are the topics covered in this review. The constant effort to revamp and re-modulate the escalating of DSSC performance is of great interest.

Moreover, researchers need to focus on how this commercial technology can be further scaled up through low-cost, zero toxicity and energy-efficient mechanisms that can benefit society. Lastly, the need to identify additional robust materials that overcome the limitations of existing components is of utmost importance, which can be tackled through extensive research and studies. This study aims to understand the different and viable commercial materials that researchers can exploit to make DSSCs reach the market as soon as possible effectively. Along with the active components and a brief introduction of DSSCs, the review highlights a few examples of certain high-efficiency DSSCs using variations in different components like the photoanode, photosensitizer, and electrodes.

Along with growing electricity and power demands, it is essential to understand how we power some of our daily appliances through a renewable source of energy (Figure 3). This review also points out the commercial activities companies have incorporated using DSSCs. Along with not being extremely stable and efficient, the article elaborates on the various strategies researchers can adopt to improve device performance and stability. DSSCs being a recent and novel innovation, India has been actively researching this particular domain. Here, we can see the various components of a DSSC that are being researched by different labs in India and how each research group aims to optimize the device's capabilities. Since the majority of the photovoltaic technologies are shifting to more organic and sustainable modes, the current sources of flowers and fruits have also been elucidated with a few vital examples and much room for improvement.

It is important to note that, once these obstacles have been overcome, the road to the commercialization of DSSCs is straightforward and it is only a matter of time that this evolution of DSSCs becomes a reality.

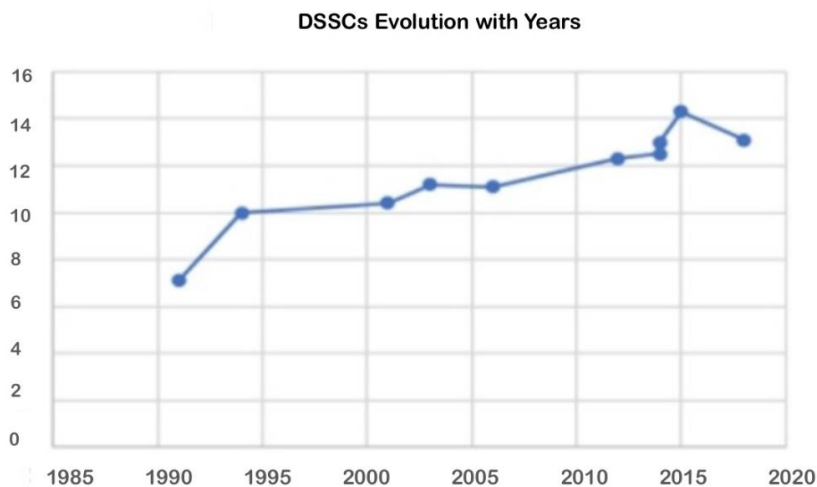


Figure 3. DSSCs Improvement over Years



ACKNOWLEDGEMENTS

I want to thank Dr. S V Eswaran, Ex: Head (Chem.) and Dean (Acad.), St. Stephen's College, Delhi; Adjunct Prof. (Hony.) Deakin Univ., Australia and TDNBC, Haryana; Ex- Emer. Sci / Hony. Prof. CSIR, AcSIR, RCB-DBT.Ex-Principal, Deshbandhu College, Delhi. Hony. Prof. AICTE, Amity Univ, supported and guided me throughout this research.

References

- [1] *Dye-sensitized solar cell* - Wikipedia, 2022, Retrieved 21 May 2022, from https://en.wikipedia.org/wiki/Dye-sensitized_solar_cell
- [2] Nazeeruddin, M., Baranoff, E., & Grätzel, M, 2011, *Dye-sensitized solar cells: A brief overview*, Solar Energy, 85(6), 1172-1178, doi: 10.1016/j.solener.2011.01.018
- [3] Godfroy, M., Liotier, J., Mwalukuku, V., Joly, D., Hualmé, Q., & Cabau, L., 2021, *Benzothiadiazole-based photosensitizers for efficient and stable dye-sensitized solar cells and 8.7% efficiency semi-transparent mini-modules*, Sustainable Energy & Fuels, 5(1), 144-153, doi: 10.1039/d0se01345e.
- [4] Liu, B., Zhu, W., Zhang, Q., Wu, W., Xu, M., & Ning, Z., 2009, *Conveniently synthesized isophorone dyes for high efficiency dye-sensitized solar cells: tuning photovoltaic performance by structural modification of donor group in donor- π -acceptor system*, Chemical Communications, (13), 1766, doi: 10.1039/b820964b.
- [5] Horiuchi, Hidetoshi Miura, Kouichi Sumioka, and Satoshi Uchida, 2004, *High Efficiency of Dye-Sensitized Solar Cells Based on Metal-Free Indoline Dyes Tamotsu*, Journal of the American Chemical Society 126 (39), 12218-12219 DOI: 10.1021/ja0488277
- [6] Ji, J.-M., Zhou, H., Eom, Y. K., Kim, C. H., Kim, H. K., 2020, *14.2% Efficiency Dye-Sensitized Solar Cells by Co-sensitizing Novel Thieno[3,2-b]indole-Based Organic Dyes with a Promising Porphyrin Sensitizer*, Adv. Energy Mater, 10, 2000124, <https://doi.org/10.1002/aenm.202000124>.
- [7] Joly, D., Pellejà, L., Narbey, S., Oswald, F., Chiron, J., & Clifford, J., 2014, *A Robust Organic Dye for Dye Sensitized Solar Cells Based on Iodine/Iodide Electrolytes Combining High Efficiency and Outstanding Stability*, Scientific Reports, 4(1), doi: 10.1038/srep04033.
- [8] Zhang, D., Stojanovic, M., Ren, Y., Cao, Y., Eickemeyer, F., & Socie, E., 2021, *A molecular photosensitizer achieves a Voc of 1.24 V enabling highly efficient and stable dye-sensitized solar cells with copper(II/I)-based electrolyte*, Nature Communications, 12(1), doi: 10.1038/s41467-021-21945-3.
- [9] Chen, H., Xie, Y., Cui, H., Zhao, W., Zhu, X., & Wang, Y., 2014, *In situ growth of a MoSe₂/Mo counter electrode for high efficiency dye-sensitized solar cells*, Chem. Commun., 50(34), 4475-4477, doi: 10.1039/c3cc49600g.



- [10] Mao, X., Zhou, R., Zhang, S., Ding, L., Wan, L., & Qin, S., 2016, *High Efficiency Dye-sensitized Solar Cells Constructed with Composites of TiO₂ and the Hot-bubbling Synthesized Ultra-Small SnO₂ Nanocrystals*, *Scientific Reports*, 6(1), doi: 10.1038/srep19390.
- [11] Xiang, W., Huang, W., Bach, U., & Spiccia, L, 2013, *Stable high efficiency dye-sensitized solar cells based on a cobalt polymer gel electrolyte*, *Chemical Communications*, 49(79), 8997, doi: 10.1039/c3cc44555k.
- [12] Boschloo, G, 2019, *Improving the Performance of Dye-Sensitized Solar Cells*, *Frontiers In Chemistry*, 7, doi: 10.3389/fchem.2019.00077.
- [13] *Approaches to Improve Efficiency of Dye-Sensitized Solar Cells* | Журнал "Макрогетероциклы", (2022), Retrieved 5 May 2022, from <https://macroheterocycles.isuct.ru/en/mhc160752e>.
- 14 Ezhov, Artem & Zhdanova, Kseniya & Bragina, Natalya & Mironov, Andrey, 2016, *Approaches to Improve Efficiency of Dye-Sensitized Solar Cells*, *Macrocycles*, 9, 337-352, 10.6060/mhc160752e
- [15] *Complete Solid-State Dye-Sensitized Solar Cell*, 2022, Retrieved 5 May 2022, from https://www.ricoh.com/technology/tech/066_dssc.
- [16] *Bloomberg - Are you a robot?*, 2022, Retrieved 5 May 2022, from <https://www.bloomberg.com/news/articles/2021-07-07/self-charging-headphones-use-solar-cells-to-keep-music-blaring>
- [17] *World's first commercial application of DSSC solar technology is in the bag*, 2009, Retrieved 5 May 2022, from <https://newatlas.com/first-commercial-application-dssc-solar-technology/13100/>
- [18] *Dye Sensitized Solar Cell Market Growth Report 2020-2027*, 2022, Retrieved 5 May 2022, from <https://www.grandviewresearch.com/industry-analysis/dye-sensitized-solar-cell-market>
- [19] Admin, 2022, *3gsolar*, Retrieved 5 May 2022, from <https://www.3gsolar.com/>
- [20] RE Partner Solution, 2022, *SHARP Dye-Sensitized Solar Cell*, Retrieved 5 May 2022, from <https://www.renesas.com/us/en/document/prb/sharp-dye-sensitized-solar-cell-renesas-re-partner-solution>
- [21] Fujikura, *Europe Ltd > 2G HTS wire*, 2022, Retrieved 5 May 2022, from <https://www.fujikura.co.uk/products/energy-and-environment/dye-sensitized-solar-cell/>
- [22] Godibo, Desalegn J., Anshebo, Sisay T., & Anshebo, Teketel Y., 2015, *Dye Sensitized Solar Cells Using Natural Pigments from Five Plants and Quasi-Solid State Electrolyte*, *Journal of the Brazilian Chemical Society*, 26(1), 92-101, <https://doi.org/10.5935/0103-5053.20140218>
- [23] Ung, M. C. ., Sipaut, C. S. ., Dayou, J. ., Liow, K. S. ., Kulip, J. ., & F. Mansa, R., 2021, *Study on Fruit Based Dye Sensitized Solar Cell*, *Recent Trends in Chemical and Material Sciences* Vol. 4, 88–93, <https://doi.org/10.9734/bpi/rtcams/v4/13663D>